J. Civil Eng. Mater.App. 2021 (December); 5(4): 197-210

Journal of Civil Engineering and Materials Application

Journal home page: http://jcema.com

Received: 17 October 2021 • Accepted: 03 December 2021

Research

doi: 10.22034/JCEMA.2021.143385

Study of the Effect of Fiber Reinforced Concrete (FRC) Enclosed with Fiber Reinforced Polymers on the Column under Finite Element Analysis

Seyed Ali Mousavi Davoudi

Department of Civil Engineering, Tabari University of higher Education, Babol, Iran.

*Correspondence should be addressed to Seyed Ali Mousavi Davoudi, Department of Civil Engineering, Tabari University of higher Education, Babol, Iran. Tel: +989112135016; Fax: +981132662426; Email: Ali_mousavii@yahoo.com.

ABSTRACT

Composite columns are columns consisting of a base section and one or more reinforcing sections (filler or filler). The components of a composite do not combine chemically so that the components fully retain their chemical and natural nature, and there is a certain common surface between the components. In terms of the reinforcing section, composites are divided into fiber-reinforced composites (FRC) and particle-reinforced composites (PRC). FRP composite profiles are composite materials that are obtained from carbon, glass, or aramid fibers embedded in a polymer resin (epoxy resin or polyester resin) and as a suitable alternative for areas where the use of steel profiles due to severe corrosion and Or the existence of strong magnetic fields is impossible. Common composite columns are a combination of concrete and composite steels, including FRP rebars and other types of composite rebars. In this research, the study of structural columns made of fiber reinforced concrete (FRP) surrounded by fiber-reinforced polymers (FRC) is presented. Modeling will be performed using Abaqus finite element software. After performing numerical analysis, it was found that fiber concrete has a better and better functional behavior than the column with ordinary concrete, and also, the effect of reinforced fibers increases the compressive strength of the column.

Keywords: Concrete Column, FRC Fiber Reinforced Concrete, Polymer Fiber, Finite Element Analysis.

1. INTRODUCTION

Concrete is a material that many of its properties can be improved by changing or improving the properties of its separate components. The basis of concrete components is cement, aggregate, and water. Gradually, more compatibility with higher types of cement and alternative materials can be achieved with higher quality [1]. Fiber-reinforced concrete is a type of fiber-reinforced concrete that has increased the structural integrity of the concrete. Fiber concrete contains short, discrete, evenly distributed, randomly oriented, and inclined fibers. The fibers in this type of concrete are steel fibers, glass fibers, synthetic fibers, and natural fibers, each of which has a different property for concrete. In addition, the behavior of fiber-reinforced concrete varies depending on density, orientation, distribution, geometric shape, and fiber material. The use of fibers as a reinforcing material is not a new topic and has been used since ancient times. Asbestos fibers have been used in concrete since the 1900s. In the 1950s, the concept of composite materials was introduced, and the issue of fiber concrete was first considered [2].

Figure 1. View of fiber concrete

From 1960, a new type of concrete entered the industrial field. This type of concrete has been used separately with random distribution as a new part in addition to ordinary concrete parts, and the tensile and shear strength of fibrous concrete is higher than ordinary concrete. In addition, fiber concrete performs much better performance against dynamic loads such as earthquakes and shocks due to its good energy absorption properties. Unlike ordinary concrete, these materials are able to withstand considerable tensile stresses and strains at tensile loads and can be used in design [3]. Over the past two decades, a variety of fiber-reinforced polymer composites (FRP) for the reinforcement and improvement of structures has been one of the newest applied achievements of civil engineering in the world today. Due to their special advantages, such as the high tensile capacity to specific gravity and excellent corrosion resistance, they were gradually accepted [4]. FRP reinforced polymer fibers can be used to repair or reinforce and improve all types of concrete structures by mounting on the surface (slabs and beams, columns, load-bearing walls, trusses, and foundations) and in residential, office, and commercial buildings, industrial buildings, machine supports. And it used heavy installations, water structures such as dams, canals, ditches, etc., road and rail stairs, water and fluid reservoirs and reservoirs, silos, and cooling towers. (Smith, 2012) With the advancement of science and technology, construction experts try to achieve the technology of construction of new materials that, in addition to performing tasks considered in other aspects affecting the structure such as weight, strength, comfort, application, and length Omar also have advantages. One of these materials that has these advantages is polymer composites. These materials can be used in different ways and in different parts of the structure [5]. In recent years, FRP composites have been used for various tasks. In the past, synthetic fibers such as glass, carbon, plastic, and aramid have been used for anti-corrosion properties [6]. Although these materials are biodegradable and expensive in terms of environmental and financial conditions, recently, natural fibers have been used more because they do not harm the environment, including hemp fibers, coconut fiber fibers, hemp, sisal, and pineapple, and FRP composites due to their lower density and higher strength. After working with more than 20 FRP cases, the scientists concluded that fibers are the best option in terms of low cost, low weight, and high strength against impact and corrosion. (Chen and Cho, 2016) In 2017 [7], Krishna and Mateo, in an article entitled CFRP, Advanced Stretch Active Active in RCC Structures, stated that the need to reconstruct reinforced concrete structures had increased rapidly. Polymer fiber-reinforced (FRP) composite materials for relatively high-weight concrete structures can provide good performance against forces while minimizing overweight. It also has good fatigue properties and does not endanger the mental health of residents. Polymer-reinforced carbon fiber (CFRP) system is a system based on carbon fiber and epoxy resins. PF prestressing sheets are more effective materials used as part of the tensile capacity and contribute to the load-bearing capacity under final load conditions. It is an ideal method that combines the advantages of advanced stainless steel composite materials and is very light and presented in high-efficiency FRP sheets through external prestressing. An innovative mechanical anchorage system was developed to reinforce the FRP sheet directly by jacking and reacting against the RCC structure. This paper uses the CFRP sheet to strengthen the RCC structure, including practical applications in roofs and stairs [8]. In a 2016 paper, Jiang et al. Conducted an experimental study on the seismic behavior of bridges with BFRP-repaired circular columns mounted near the surface, covering the outer BFRP panels. In this paper, using BFRP, its first letter indicates (Near-surface mounted) NSM (installation near the surface) and covering BFRP plates, a fast fan for repairing earthquake-damaged columns is presented. Then, the 4 damaged columns of the bridge with hydraulic columns were repaired with the proposed techniques and tested under cyclic lateral load. The results show that the flexural capacity of the repaired columns has been restored and even increased [9].

2. METHODOLOGY

In this study, to study the effect of fiber reinforced concrete (FRC) enclosed with fiber reinforced polymers on the column under finite element analysis, four study samples with the specifications presented in Table (1) were used, all samples mentioned by the program Abaqus have been modeled and analyzed.

Table 1. Mechanical specifications of CFRP sheets

Model	Size	Height	Parameter
A	45345cm	4m	**Simple**
B			**CFRP**
C			**GFRP**
D			**BFRP**

Also in Table (2) the mechanical specifications of the CFRP sheet used in Model B are specified.

Table 2. Mechanical specifications of CFRP sheets

	Thickness (mm)	E1 (Pa)	g (Kg/m3)
CFRP	1	18E5	2200

Table (3) shows the mechanical properties of the GFRP sheet used in Model C.

Table 3. Mechanical specifications of GFRP sheets

	Thickness (mm)	E1 (Pa)	g (Kg/m3)
GFRP	1	65E5	2500

Also in Table (4) the mechanical specifications of the BFRP sheet used in Model D are specified.

Table 4. Mechanical properties of BFRP sheets

	Thickness (mm)	E1 (Pa)	g (Kg/m3)
BFRP	1	50E5	1200

Table (5) shows the mechanical properties of concrete used in modeling samples.

Table 5. Mechanical properties of fiber concrete

g/cm3	*f*t (MPa)	Ef (GPa)
2485	2788	**200**

Table (6) shows the mechanical properties of the rebar used in modeling the samples.

Table 6. Mechanical specifications of sample rebar

	u	g Kg/m^3	E (mpa)
Rebar-S400	0.3	7850	2.05E10^5

Laboratory studies of Jiaxin Chen [10] et al. In 2016 were used for software verification of the Abaqus program. The sample is very small and has a slight difference of about 15%, which is shown in the shapes of the studied sample and their stress-strain diagram.

Figure 2. View of the laboratory sample of Jiaxin Chen et al. [10]

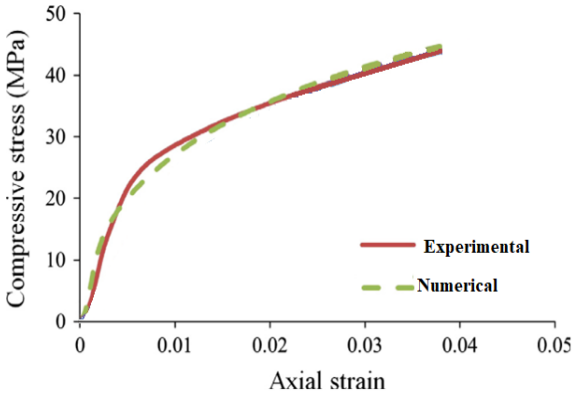

Figure 3. Validation diagram

2.1. Modelling Process

In order to model the behavior of fiber concrete, the separation behavior in Fiber Concrete Composites is used. The amount of shear stress between the fibers and concrete increases by pulling the steel strand from the concrete bed. At a certain amount of maximum shear stress, adhesion and bonding between the string and the concrete substrate begin to disappear. This is not sudden and happens gradually. Stresses are transmitted normally and without problems until the maximum stress is reached. Reaching the maximum shear stress is the beginning of the initial separation. After this point, and with the onset of separation, lower amounts of stress are transferred through the interface until the interface fails (and the separation phase is complete). In order to model this separation, a Traction Separation Law is usually required. This rule should describe the onset of damage (maximum shear stress) and the damage growth (mathematical description of the separation process). Once the damage threshold values commensurate with the separation are reached, frictional behavior will take effect and play a role. By continuing to pull the steel strand out of the concrete bed at this stage, the stresses created at the joint surface of the fibers and the ground will be affected by both friction and damage growth (a separation process). Frictional stresses continue to play a role until the steel strand is completely pulled out of the concrete bed. In order to consider this behavior due to friction at the joint surface, we must use Columb's friction. This frictional behavior considers the shear stress created between two surfaces as a fraction of the surface's vertical stress. The Contact option is selected in the Interaction module and in the Create Interaction Property section. Shells are also used to model FRP fibers.

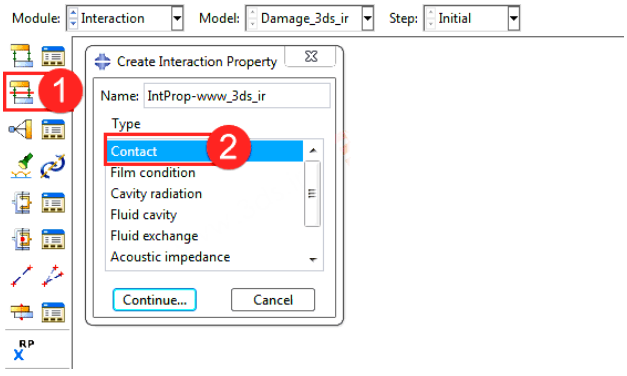

Figure 4 (a). View of the Interaction module

The Cohesive Behavior option uses the Mechanical part of Abaqus software to define the slip-bond relationship in modeling the adhesive behavior between surfaces.

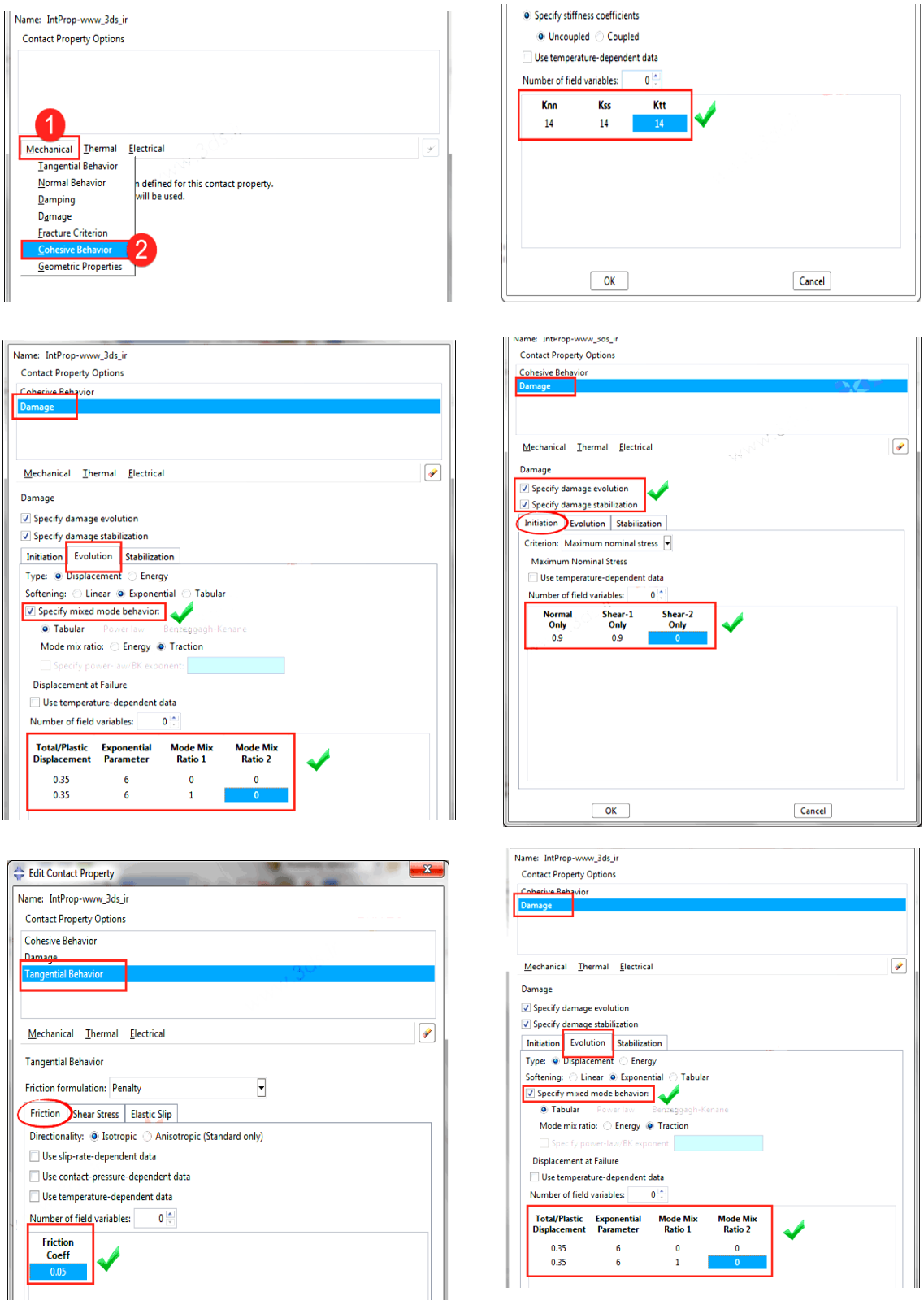

Figure 4 (b). Fiber profile in Abaqus environment

3. RESULTS AND DISCUSSION

3.1. Simple Column

In this section, simple column modeling and analysis are discussed, and the analysis results are given below. Figure (6) shows the stress distribution of Von mises in the concrete body of the column, which shows that the highest amount of Von mises stress is created at the foot of the column. It can also be seen from Figure (5) that the stress distribution of Von mises in the column rebar network has increased as it approaches the abutment. Figures (7 and 8) also show the displacement of the column in concrete and rebar, which is consistent with the expected displacement of the analysis as expected.

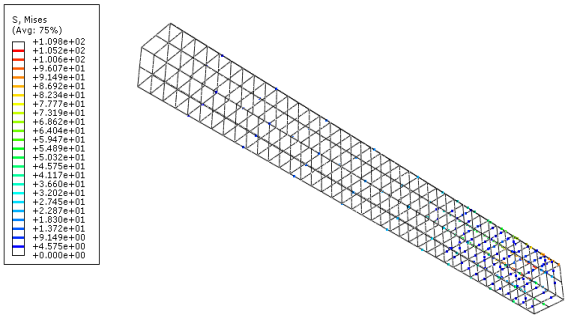

Figure 5. Von mises stress in rebars

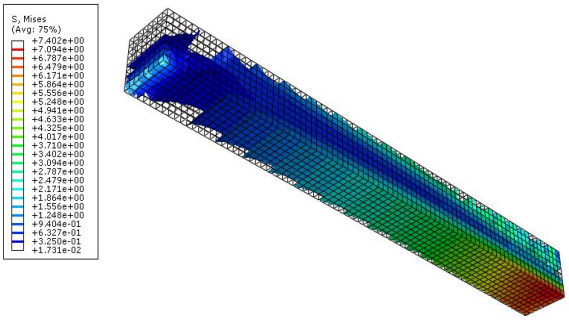

Figure 6. Von mises stress in concrete

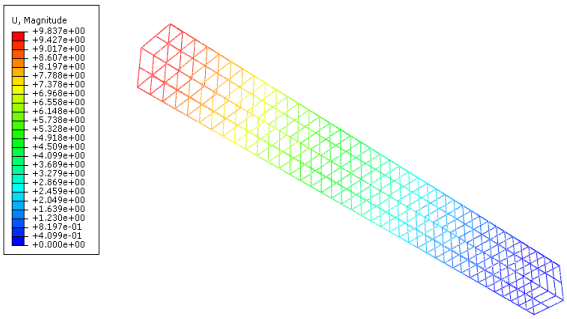

Figure 7. Displacement in the rebar

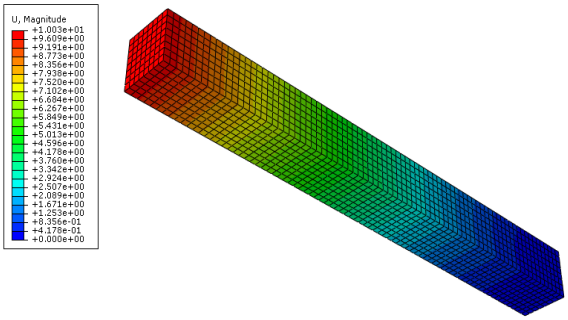

Figure 8. Displacement in the concrete

Figure 9 shows the effective strain or paste strain equivalent in the column. It can be seen that near the base of the column, there is the highest amount of paste equivalent in the tensile part of the concrete. Also, according to Figure 10, the paste strain at the base of the column in the tensile part has expanded to one-third of the column length.

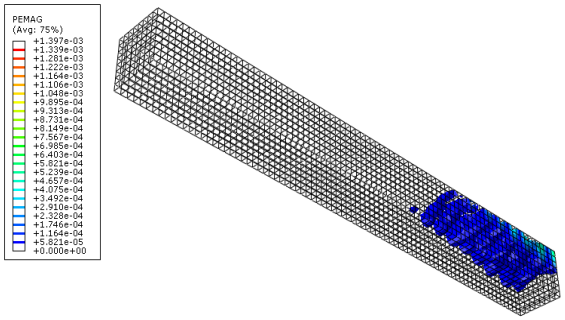

Figure 9. Magnitude of the strain

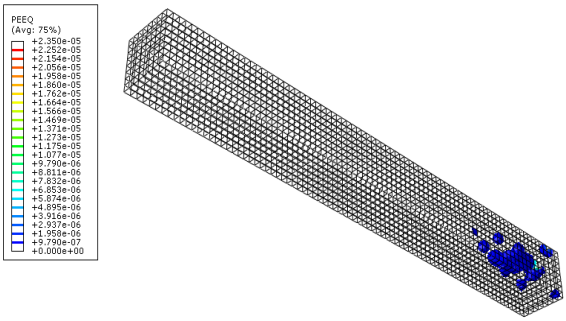

Figure 10. Effective strain

3.2. CFRP Column

In this section, modeling and analysis of columns reinforced with CFRP are discussed and the results of the analysis are given below. Figure (11) shows the stress distribution of Von mises in the concrete body of the column, which shows that the highest amount of Von mises stress is created at the foot of the column. It can also be seen from Figure (12) that the distribution of Von mises in the column rebar network has increased as it approaches the abutment. Figure (13) also shows the stress of von mises in CFRP. The compression zone at the foot of the column was the highest. Figures (15, 14, 17, and 18) also show the displacement of the column in concrete, rebar, and CFRP, which is consistent with the expected displacement and analysis of the displacement. Figure (16) shows the column's effective strain or paste equivalent. It is observed that there is the highest amount of paste equivalent formation near the base of the column, in the tensile part of the concrete, and slightly in the compressive zone. Also, according to Figure (17), the strain of the paste at the foot of the column in the tensile part has expanded to one-third of the length of the column.

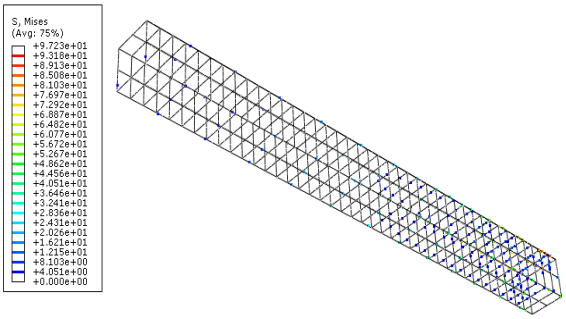

Figure 11. Von mises stress in rebars

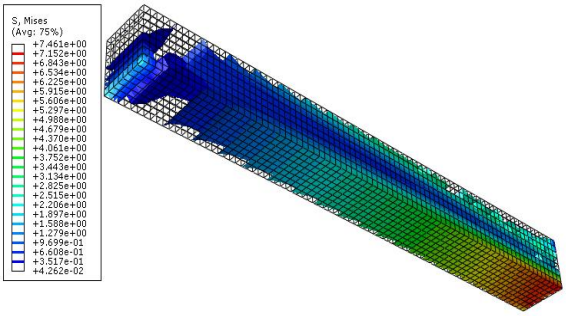

Figure 12. Von mises stress in concrete

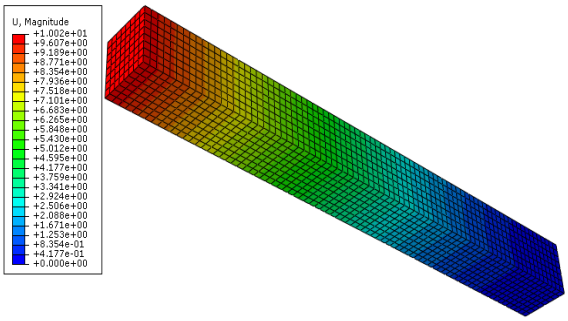

Figure 13. Von mises stress in rebars

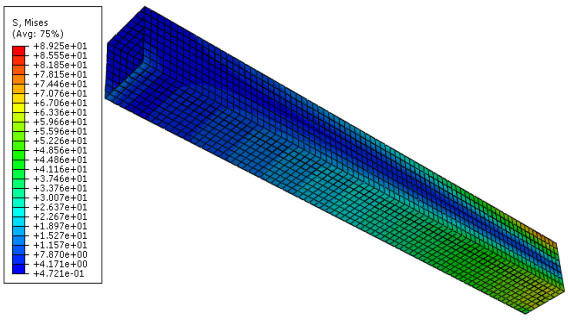

Figure 14. Von mises stress in concrete

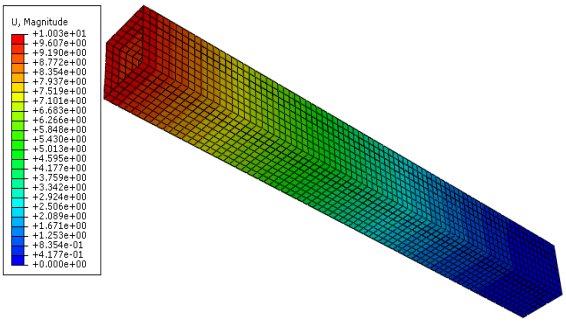

Figure 15. Displacement in the rebar

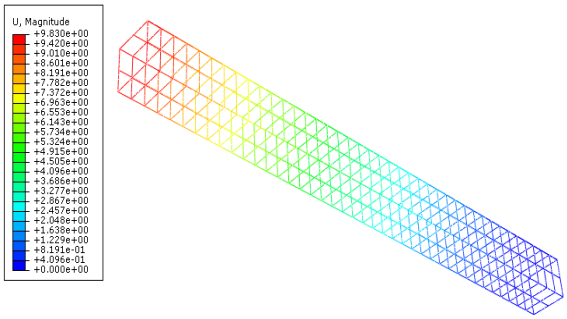

Figure 16. Displacement in the concrete

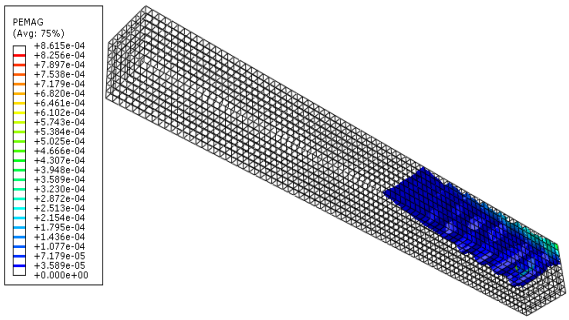

Figure 17. Magnitude of the strain

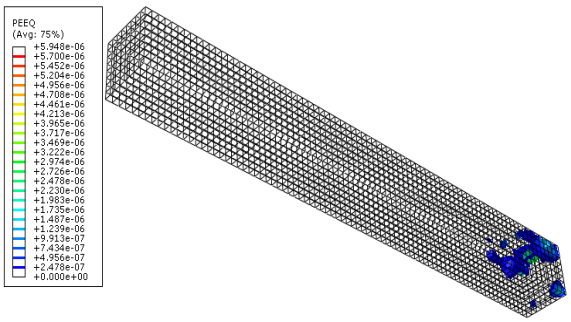

Figure 18. Effective strain

3.4. GFRP Column

In this section, modeling and analysis of columns reinforced with GFRP are discussed, and the results of the analysis are given below. Figure (19) shows the stress distribution of Von mises in the concrete body of the column, which shows that the highest amount of Von mises stress is created at the foot of the column. It can also be seen according to (Figure 20) that the stress distribution of Von mises in the column rebar network has increased as it approaches the abutment. Figure (19) also shows the stress of von mises in GFRP. The compression zone at the foot of the column was the highest. Figures (21, 22, and 23) also show the displacement of columns in concrete, rebar, and GFRP, which is consistent with the expected and constant displacement analysis. Figure (24) shows the column's effective strain or paste equivalent. It is observed that there is the highest amount of paste equivalent formation near the base of the column, in the tensile part of the concrete, and slightly in the compressive zone. Also, according to Figure (25), the strain of the paste at the foot of the column in the tensile part has expanded to one-third of the length of the column.

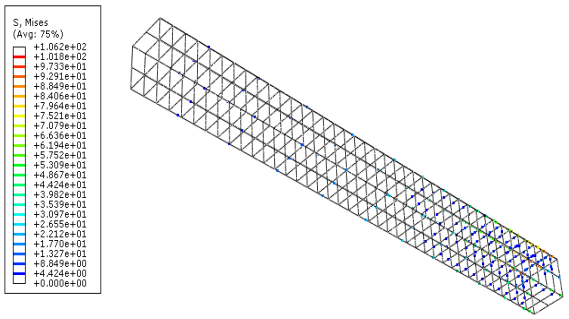

Figure 19. Von mises stress in rebars

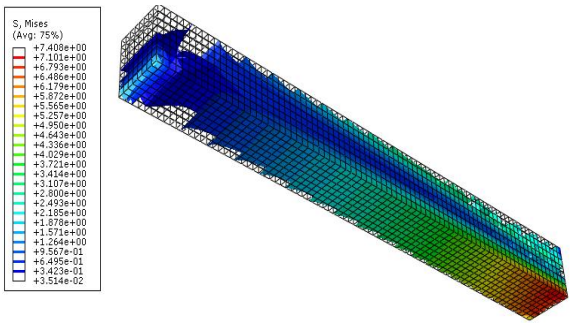

Figure 20. Von mises stress in concrete

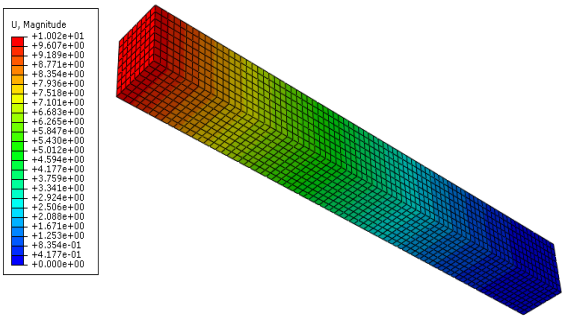

Figure 21. Stress in rebars

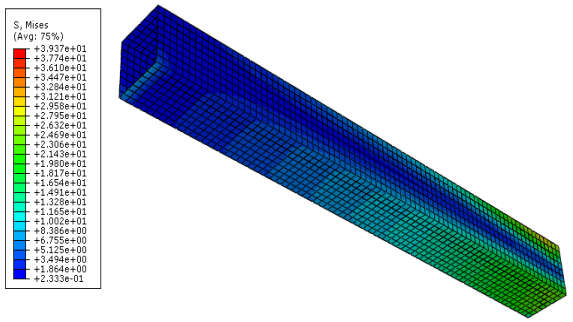

Figure 22. Von mises stress in concrete

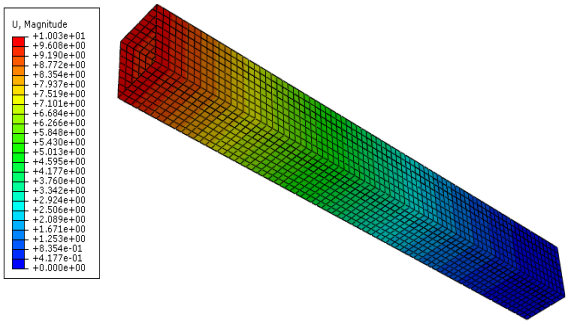

Figure 23. Displacement in the rebar

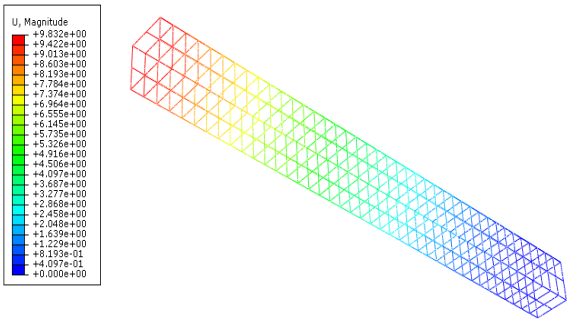

Figure 24. Displacement in the concrete

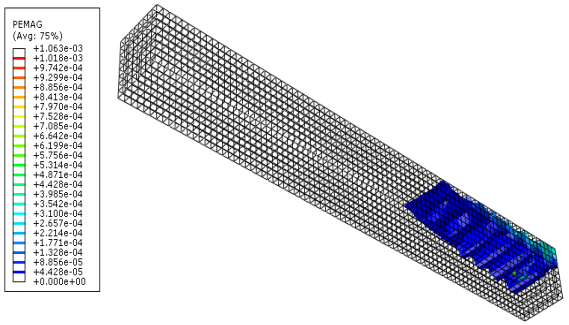

Figure 25. Magnitude of the strain

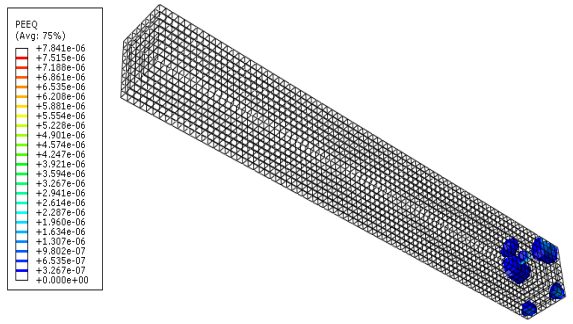

Figure 26. Effective strain

3.5. BFRP Column

In this section, modeling and analysis of BFRP-reinforced columns are performed, and the results of the analysis are given below. The greatest amount of stress is created by Von mises. It can also be seen from Figure (28) that the stress distribution of Von mises in the column rebar network has increased as it approaches the abutment. Figure (29) also shows the von Mises stress in BFRP. The compression zone at the foot of the column was the highest. Figures (30, 31, and 32) also show the displacement of the column in concrete, rebar, and BFRP, which is consistent with the expected and constant displacement analysis. Figure (33) shows the column's effective strain or paste equivalent. It is observed that there is the highest amount of paste equivalent formation near the base of the column, in the tensile part of the concrete, and slightly in the compressive zone. Also, according to Figure (34), the strain of the paste at the foot of the column in the tensile part has expanded to one-third of the length of the column.

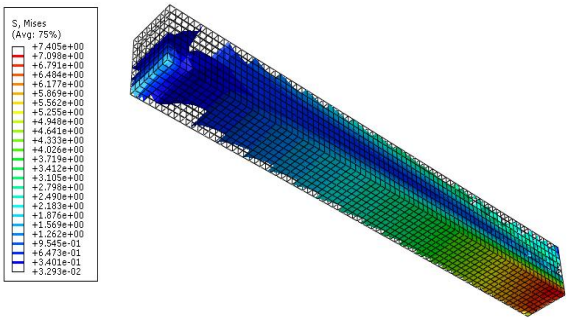

Figure 27. Von mises stress in rebars

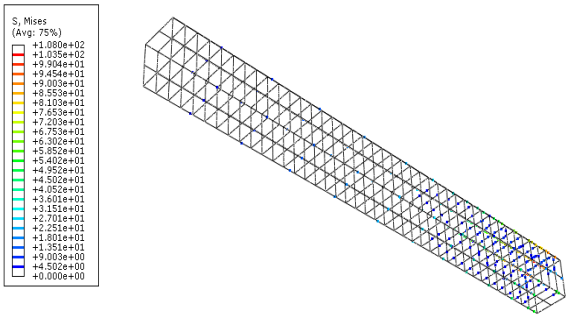

Figure 28. Von mises stress in concrete

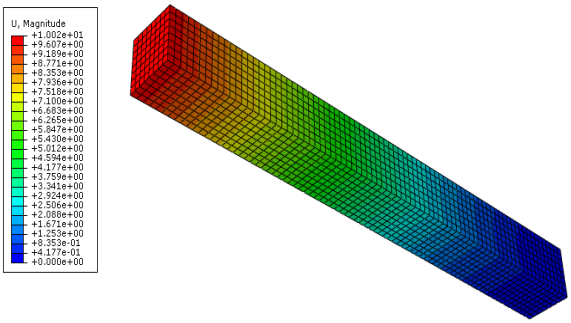

Figure 29. Von mises stress in rebars

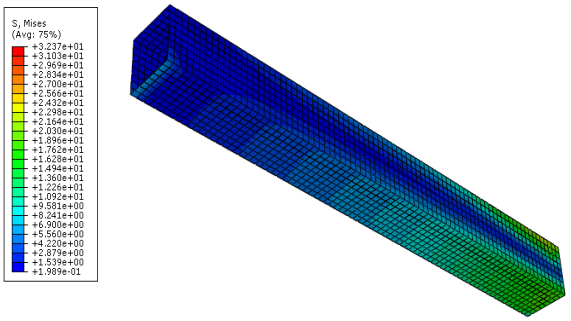

Figure 30. Von mises stress in concrete

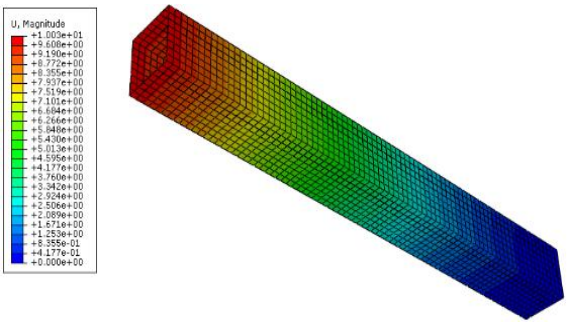

Figure 31. Displacement in the rebar

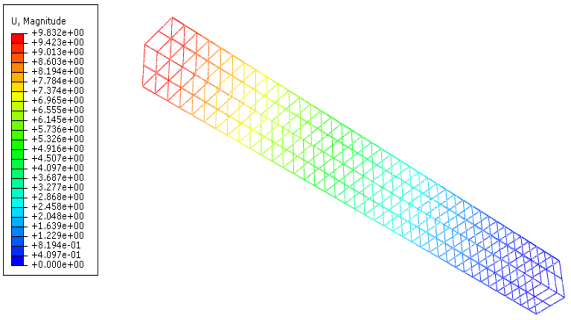

Figure 32. Displacement in the concrete

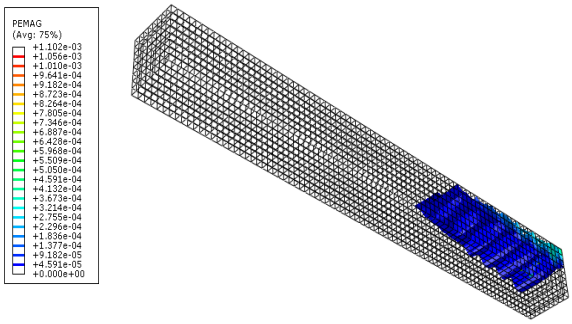

Figure 33. Magnitude of the strain

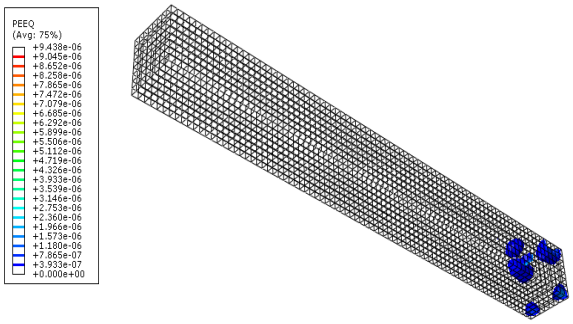

34. Effective strain

According to the analysis outputs, the research results are summarized in Table (3).

Table 3. Modeling results

Model	Maximum plastic strain	Maximum effective strain	Maximum stress Von mises in FRP (Kg/m^2)	Maximum stress Von mises in rebars (Kg/m^2)	Maximum stress Von mises in concrete (Kg/m^2)
Simpel	1.397e-3	2.35e-5	-	109.8	**7.402**
CFRP	0.8615e-3	0.5948e-5	89.25	97.23	**7.641**
GFRP	1.062e-3	0.7841e-5	39.37	106.2	**7.408**
BFRP	1.102e-3	0.9438e-5	32.37	108	**7.405**

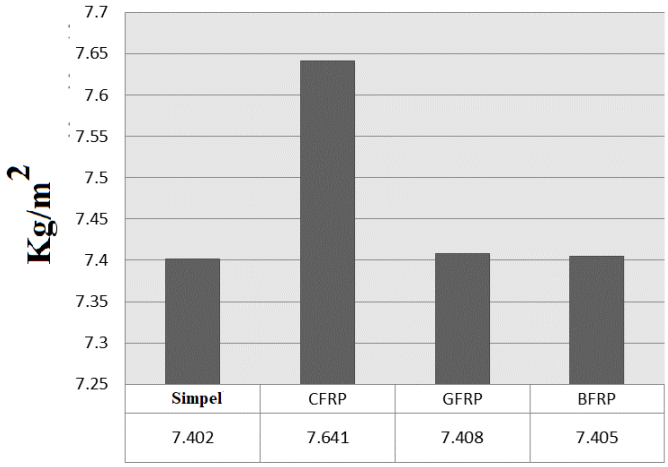

Figure 35. Comparative diagram of maximum stress of Von mises in concrete

According to Figure (35), it can be seen that the presence of CFRP reinforcement due to the carbon structure has caused the highest von Mises stress in concrete and the simple column has the lowest stress. This amount of decrease and increase of stress means to increase and decrease of displacement of column components. That is, the simple column, the column with BFRP, the column with GFRP, and the column with CFRP had the most component displacement, respectively.

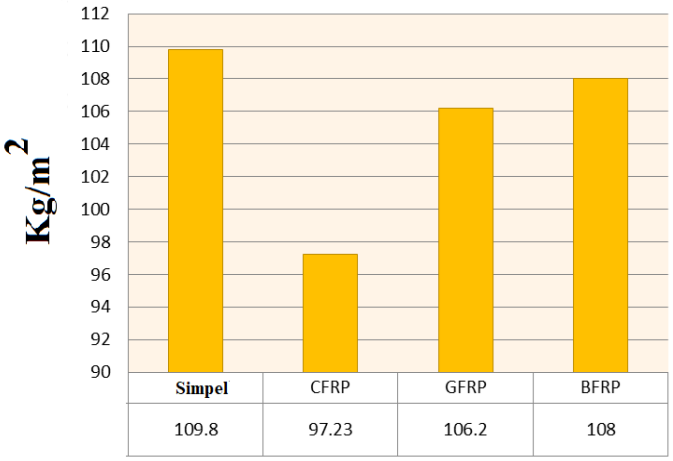

Figure 36. Comparative diagram of maximum stress of Von mises in rebar

According to Figure (36), it can be seen that the presence of CFRP amplifier due to the carbon structure caused the least von Mises stress in the rebar, and the simple column had the highest stress. Therefore, columns with CFRP, columns with BFRP, columns with GFRP, and simple columns had the most displacement of rebar components, respectively.

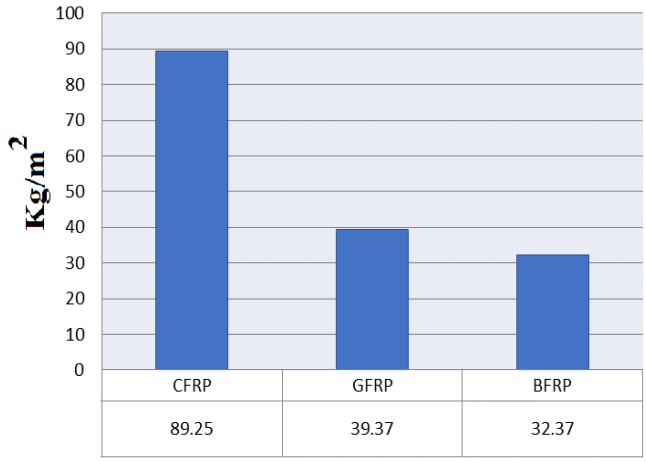

Figure 37. Comparative diagram of maximum stress of Von mises in FRP

According to Figure (37), it can be seen that the presence of CFRP amplifier caused the most stress Von mises in the composite, and the column with BFRP also had the highest stress. Therefore, columns with CFRP, columns with BFRP, columns with GFRP, and simple columns, respectively, had the least displacement of composite components.

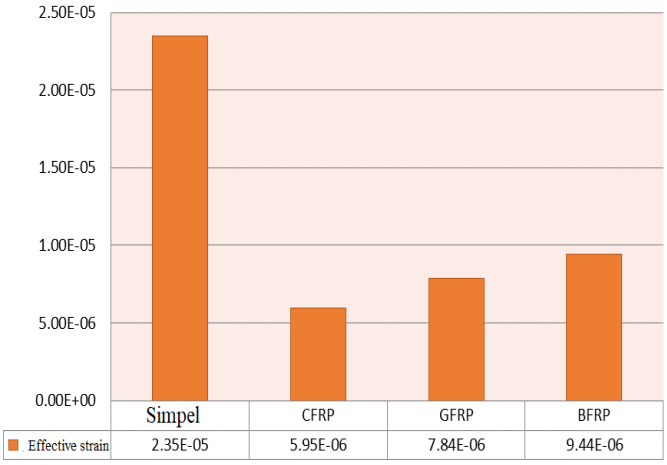

Figure 38. Comparative diagram of the effective maximum strain

According to Figure (38), it can be seen that the presence of CFRP amplifier caused the least effective strain in the column and simple column without composite amplifier had the highest effective strain. Therefore, columns with CFRP, columns with GFRP, columns with BFRP, and simple columns, respectively, had the least effective strain.

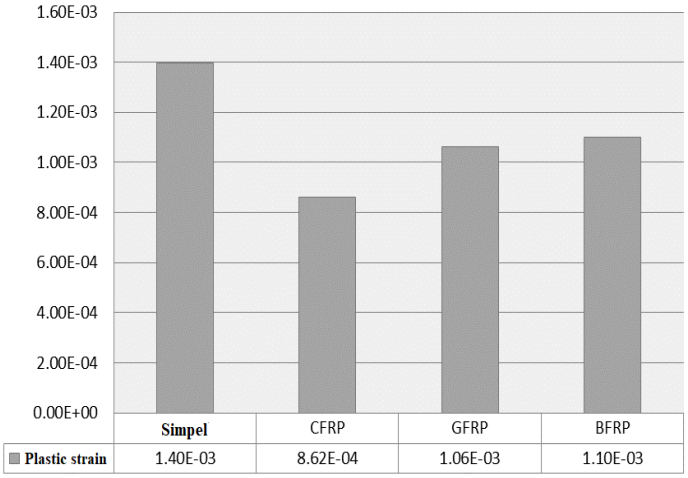

Figure 39. Comparative diagram of maximum plastic strain

According to Figure (40), it can be seen that the presence of CFRP amplifier has caused the least amount of paste strain in the column, and simple column without composite amplifier has had the highest amount of paste strain. Therefore, the column with CFRP, the column with FGFRP, the column with BFRP, and the simple column had the lowest paste strain, respectively. According to Figure (41) to Figure (43), it can be seen that by comparing ordinary concrete and FRC concrete for simple samples, CFRP, GFRP, BFRP are observed. They had the lowest dough strain, respectively.

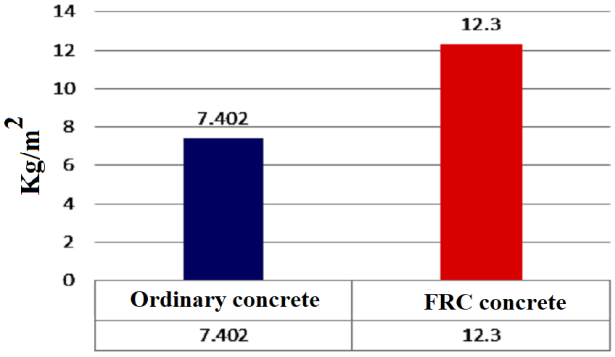

Figure 40. Comparative diagram of maximum stress of Von mises (simple model) in ordinary concrete and FRC

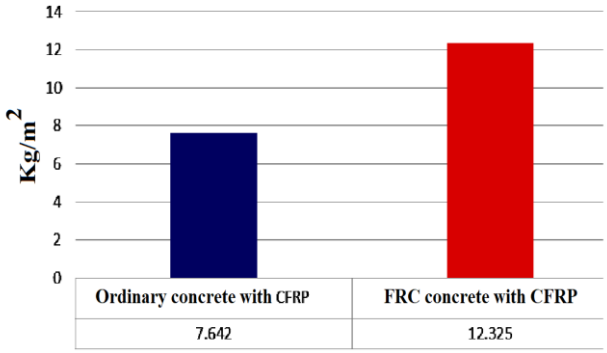

Figure 41. Comparative graph of maximum stress of Von mises (CFRP model) in ordinary concrete and FRC

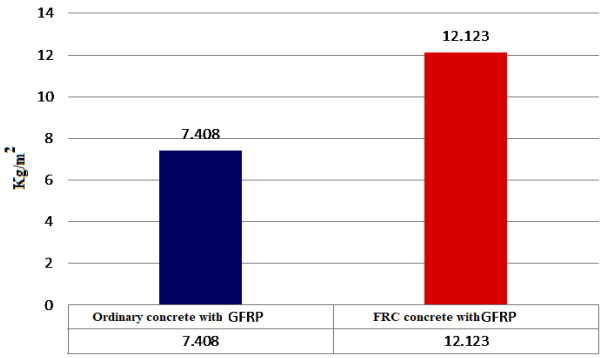

Figure 42. Comparative diagram of maximum stress of Von mises (GFRP model) in ordinary concrete and FRC

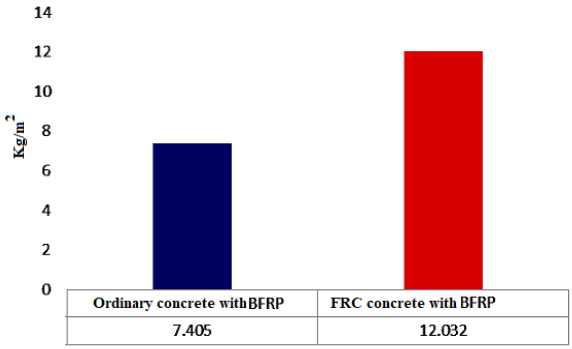

Figure 43. Comparative diagram of maximum stress of Von mises (BFRP model) in ordinary concrete and FRC

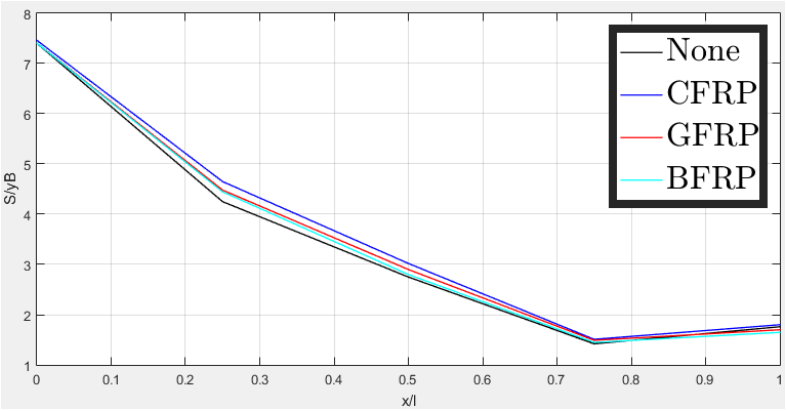

Figure 44. Parametric comparative diagram of stress distribution along the column body

Figure (44) shows the ratio of stress changes along the column from the top of the column (X / L = 0) to the bottom support (X / L = 1). According to this diagram, it can be seen that CFRP, GFRP, and BFRP composites cause more stress in the column body, which means that the column deformation is reduced. It is also observed that during the column at 0.75 feet of the column, a behavioral change occurred in the amount of column stress.

4. CONCLUSION

According to the analysis, it can be said that:

- In a simple column, near the base of the column and in the tensile part of concrete, the highest amount of dough equivalent is formed.
- In columns with composite, near the base of the column and in the tensile part of the concrete and a little in the compression zone, the highest amount of paste equivalent formation occurs.
- In columns reinforced with CFRP, GFRP, and BFRP composites, the highest stress is created in the column body, respectively.

A simple column, a column with BFRP, a column with GFRP, and a column with CFRP have the most displacement of components, respectively.

- CFRP reinforcement due to the carbon structure has caused the least stress Von mises in the rebar, and the simple column also causes the highest stress.
- CFRP column, BFRP column, GFRP column, and simple column have the most displacement of rebar components, respectively.
- The presence of a CFRP amplifier has caused the most Von mises to stress in the composite, and the column with BFRP also has the highest stress.
- Column with CFRP, a column with BFRP, a column with GFRP, and a simple column has the least displacement of composite components, respectively.
- Column with CFRP, a column with GFRP, a column with BFRP, and a simple column, respectively, had the least effective strain.
- Column with CFRP, a column with GFRP, a column with BFRP, and a simple column has the lowest plastic strain, respectively.
- It was observed in columns with FRC concrete compared to columns with ordinary concrete which were observed in simple columns and CFRP, GFRP, BFRP. This value was about 48% on average in all samples.

FUNDING/SUPPORT

Not mentioned any Funding/Support by authors.

ACKNOWLEDGMENT

Not mentioned by authors.

AUTHORS CONTRIBUTION

This work was carried out in collaboration among all authors.

CONFLICT OF INTEREST

The author (s) declared no potential conflicts of interests with respect to the authorship and/or publication of this paper.

5. REFERENCES

[1] Smith ST, Teng JG. FRP-strengthened RC beams. I: review of debonding strength models. Engineering structures. 2002 Apr 1;24(4):385-95. [View at Google Scholar]; [View at Publisher].

[2] Krishna MR, Mathew A. EFFECT OF CFRP WRAPPING IN DUCTILE BEHAVIOUR OF RCC BEAM COLUMN JOINT UNDER CYCLIC LOADING. International Research Journal of Engineering and Technology (IRJET). 2017;4(5):1360-3. [View at Google Scholar]; [View at Publisher].

[3] Chen J, Chouw N. Compressive behaviour of flax FRP double tube confined coconut fibre reinforced concrete. Construction and Building Materials. 2016 Jun 1;112:666-73. [View at Google Scholar]; [View at Publisher].

[4] Jiang SF, Zeng X, Shen S, Xu X. Experimental studies on the seismic behavior of earthquake-damaged circular bridge columns repaired by using combination of near-surface-mounted BFRP bars with external BFRP sheets jacketing. Engineering Structures. 2016 Jan 1;106:317-31. [View at Google Scholar]; [View at Publisher].

[5] Thomas A. Sprayed concrete lined tunnels. CRC Press; 2008 Oct 8. [View at Google Scholar]; [View at Publisher].

[6] Awang H, Ahmad MH. The effect of steel fibre inclusion on the mechanical properties and durability of lightweight foam concrete. Adv. Eng. Inform. 2012 Jun 15;48:9348-51. [View at Google Scholar]; [View at Publisher].

[7] Hadigheh SA, Mahini SS, Maheri MR. Seismic behavior of FRP-retrofitted reinforced concrete frames. Journal of Earthquake Engineering. 2014 Nov 17;18(8):1171-97. [View at Google Scholar]; [View at Publisher].

[8] Wang W, Sheikh MN, Hadi MN, Gao D, Chen G. Behaviour of concrete-encased concrete-filled FRP tube (CCFT) columns under axial compression. Engineering Structures. 2017 Sep 15;147:256-68. [View at Google Scholar]; [View at Publisher].

[9] Cao Y, Wu YF, Jiang C. Stress-strain relationship of FRP confined concrete columns under combined axial load and bending moment. Composites Part B: Engineering. 2018 Feb 1;134:207-17. [View at Google Scholar]; [View at Publisher].

[10] Vasiliev VV, Morozov EV. Advanced mechanics of composite materials and structural elements. Newnes; 2013 Jun 19. [View at Google Scholar]; [View at Publisher].

[11] Jones BD, Thomas AH, Hsu YS, Hilar M. Evaluation of innovative sprayed-concrete-lined tunnelling. Proceedings of the Institution of Civil Engineers-Geotechnical Engineering. 2008 Jun;161(3):137-49. [View at Google Scholar]; [View at Publisher].

[12] Hales TA, Pantelides CP, Reaveley LD. Analytical buckling model for slender FRP-reinforced concrete columns. Composite Structures. 2017 Sep 15;176:33-42. [View at Google Scholar]; [View at Publisher].

[13] Hadi MN. Comparative study of eccentrically loaded FRP wrapped columns. Composite structures. 2006 Jul 1;74(2):127-35. [View at Google Scholar]; [View at Publisher].

[14] Teng, J.G.; Chen, J.F.; Smith, S.T.; and Lam, L.; "FRP - strengthened RC structures", Wiley, West Sussex, U.K, 2002. [View at Google Scholar]; [View at Publisher].

[15] Eid R, Paultre P. Compressive behavior of FRP-confined reinforced concrete columns. Engineering Structures. 2017 Feb 1;132:518-30. [View at Google Scholar]; [View at Publisher].

[16] Moretti ML, Arvanitopoulos E. Overlap length for confinement of carbon and glass FRP-jacketed concrete columns. Composite Structures. 2018 Jul 1;195:14-25. [View at Google Scholar]; [View at Publisher].

[17] Bai J, editor. Advanced fibre-reinforced polymer (FRP) composites for structural applications. Elsevier; 2013 Sep 30.[View at Google Scholar]; [View at Publisher].

[18] Zeng XG, Jiang SF, Xu XC, Huang HS. Numerical modeling of earthquake-damaged circular bridge columns repaired using combination of near-surface-mounted BFRP bars with external BFRP sheets jacketing. Materials. 2019 Jan;12(2):258. [View at Google Scholar]; [View at Publisher].

[19] Chen J, Chouw N. Flexural behaviour of flax FRP double tube confined coconut fibre reinforced concrete beams with interlocking interface. Composite Structures. 2018 May 15;192:217-24. [View at Google Scholar]; [View at Publisher].

[20] Miracle DB, Donaldson SL, Henry SD, Moosbrugger C, Anton GJ, Sanders BR, Hrivnak N, Terman C, Kinson J, Muldoon K, Scott Jr WW. ASM handbook. Materials Park, OH: ASM international; 2001 Jan. [View at Google Scholar]; [View at Publisher].

[21] Karbhari VM, Gao Y. Composite jacketed concrete under uniaxial compression—Verification of simple design equations. Journal of materials in civil engineering. 1997 Nov;9(4):185-93. [View at Google Scholar]; [View at Publisher].